Compact all-fiber quartz-enhanced photoacoustic spectroscopy sensor with a 30.72 kHz quartz tuning fork and spatially resolved trace gas detection

Yufei Ma,[1,2,a)] Ying He,[1] Xin Yu,[1] Jingbo Zhang,[1] Rui Sun,[2] and Frank K. Tittel[3]
[1]*National Key Laboratory of Science and Technology on Tunable Laser, Harbin Institute of Technology, Harbin 150001, China*
[2]*Post-doctoral Mobile Station of Power Engineering and Engineering Thermophysics, Harbin Institute of Technology, Harbin 150001, China*
[3]*Department of Electrical and Computer Engineering, Rice University, 6100 Main Street, Houston, Texas 77005, USA*

(Received 4 February 2016; accepted 23 February 2016; published online 4 March 2016)

An ultra compact all-fiber quartz-enhanced photoacoustic spectroscopy (QEPAS) sensor using quartz tuning fork (QTF) with a low resonance frequency of 30.72 kHz was demonstrated. Such a sensor architecture has the advantages of easier optical alignment, lower insertion loss, lower cost, and more compact compared with a conventional QEPAS sensor using discrete optical components for laser delivery and coupling to the QTF. A fiber beam splitter and three QTFs were employed to perform multi-point detection and demonstrated the potential of spatially resolved measurements.
 [http://dx.doi.org/10.1063/1.4943233]

Laser based trace gas sensing methods are widely used in many applications, such as atmospheric chemistry,[1] industrial process control and combustion diagnostics,[2] as well as medical diagnostics and the life sciences,[3] due to their high detection sensitivity and selectivity. Among these methods, photoacoustic spectroscopy (PAS) is one of the most effective trace gas detection technologies. PAS employs a broadband microphone for acoustic wave detection and is characterized by a low cost and robust architecture. However, most microphone-based PAS cells have a low resonance frequency, which makes PAS cells more sensitive to environmental and sample gas flow noise. Moreover, the size of a typical photoacoustic cell is relatively large.[4]

Quartz-enhanced photoacoustic spectroscopy (QEPAS) technique[5] is a significant improvement of the microphone-based PAS method. QEPAS uses low cost, commercially available millimeter sized piezoelectric quartz tuning forks (QTFs) as acoustic wave transducers which possesses high selectivity and immunity to ambient acoustic noise.[6–8] In QEPAS technology, the acoustic energy is accumulated in the sharply resonant QTF instead of a large photoacoustic cell as in conventional PAS. Therefore, the limitation of gas cell size no longer exists and the cell volume can be reduced, and even the cell can be optional.

In QEPAS, usually an optical fiber collimator and focusing lens are used for laser delivery and coupling.[9–11] An all-fiber configuration has the advantages of easier optical alignment, lower insertion loss, reduction in sensor size, and lower cost. To-date, QEPAS has not been applied to multi-point detection and spatially resolved trace gas concentration measurements.

In this work, a single mode fiber was used for laser delivery to construct an ultra compact all-fiber QEPAS sensor system. In addition, a fiber beam splitter (FBS) was employed to split the laser beam into three branches, which resulted in three point QTF based gas detection and demonstrated multi-point detection and spatially resolved trace gas concentration measurements.

Commercially available QTFs with a resonant frequency f_0 of ~32.76 kHz are usually used in QEPAS sensors. The QEPAS signal amplitude is inversely proportional to the QTF resonance frequency. A QTF with a smaller f_0 will result in a longer effective integration time, which increases the QEPAS signal. In this paper, a QTF with f_0 of 30.72 kHz was used as an acoustic wave transducer. The length, width, and thickness of the QTF prongs and the gap spacing between the two prongs are listed in Table I.

The experimental sensor system is shown in Fig. 1. Water vapor (H_2O) was chosen as the target analyte. A 1.395 μm continuous wave, distributed feedback (CW-DFB) fiber-coupled diode laser was employed as the laser excitation source. The diode laser output was divided in a 1:1:1 ratio by means of a single mode FBS for the three all-fiber QEPAS sensor system with three QTFs. The single mode fiber employed in the sensing platform has a length of 3 m, a core diameter of 8.2 μm, and an insertion loss of <0.3 dB. The fiber end was placed on an adjustable base which can be varied in the x, y, and z directions. The fiber output was placed close to the QTF prongs without an optical focusing lens. The distance between the laser output and the QTF prongs was 300 μm, and the beam diameter at the center of the QTF was ~100 μm. Modulation of the laser current was implemented by applying a sinusoidal dither to the direct current ramp of the diode laser at half of the QTF resonance frequency ($f = f_0/2$). The piezoelectric signal generated by the QTF was detected by a low noise transimpedance amplifier with a 10 MΩ feedback resistor and converted into a voltage. Subsequently, this voltage was transferred to a

TABLE I. Parameters of geometries for QTF.

QTF with f_0 (kHz)	Length (mm)	Width (mm)	Thickness (mm)	Gap (mm)
30.72	3.9	0.62	0.36	0.32

a)Electronic mail: mayufei@hit.edu.cn

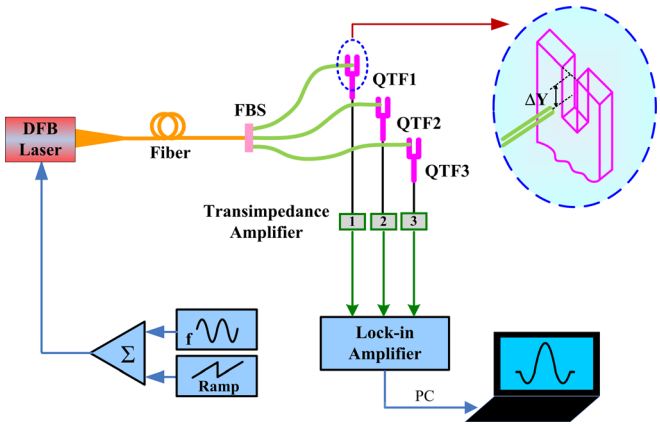

FIG. 1. Schematic configuration of an all-fiber QEPAS sensor system.

lock-in amplifier for a measurement of the 2*f* component generated by the QTF.

Laboratory air was employed as the target analyte which contained 0.46% H_2O as determined by means of a tunable diode laser absorption spectroscopy (TDLAS) method.[12] The H_2O absorption line located at 7168.4 cm^{-1} was selected for laser excitation and the laser power for each sensor branch was ~4.83 mW. The all-fiber QEPAS sensor performance using the three QTFs with f_0 of 30.72 kHz was evaluated. The impact of ΔY (see Fig. 1 inset) between the laser beam and the top of QTF prongs on QEPAS signal level was investigated, and the experimental results are shown in Fig. 2. The modulation depth of laser wavelength was set to 0.39 cm^{-1}. The 2*f* QEPAS signal amplitude increased rapidly with ΔY when it was <0.6 mm. The peak region of the 2*f* signal amplitude occurred in the range of ΔY from 0.6 mm to 1 mm. With a further increase of ΔY, the signal amplitude decreased due to the more challenging QTF prong vibration when the acoustic wave source is at the bottom of the QTF prongs. At ΔY of 0.8 mm, the 2*f* QEPAS signal amplitude was 163.2 mV, 166.6 mV, and 171.3 mV for QTF1, QTF2, and QTF3, respectively. The small differences of signal response among the three sensors mainly resulted from small differences of the three QTFs such as the Q-factor. In the following experiments, the optimum value of ΔY of 0.8 mm was chosen to achieve the maximum QEPAS signal amplitude.

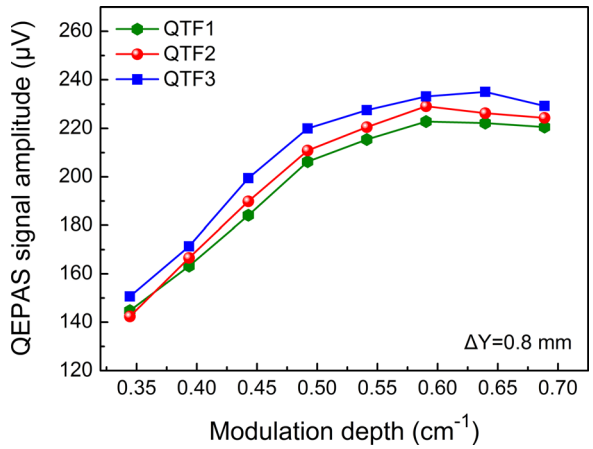

FIG. 3. All-fiber QEPAS signal amplitude as a function of modulation depth at ΔY of 0.8 mm for three QTF sensors.

The laser wavelength modulation depth was optimized in order to improve the 2*f* QEPAS signal amplitude. The dependence of the all-fiber QEPAS signal amplitude as a function of the laser wavelength modulation depth is depicted in Fig. 3. The all-fiber QEPAS signal amplitude increased with the modulation depth, but when the modulation depth was >0.59 cm^{-1}, no further significant change was observed. Therefore, a modulation depth of 0.59 cm^{-1} was found to be optimum.

The measured 2*f* QEPAS signal and noise at a modulation depth of 0.59 cm^{-1}, and ΔY of 0.8 mm for the three QTFs is shown in Fig. 4. The signal amplitude was 222.9 mV, 229.2 mV, and 233.2 mV for QTF1, QTF2, and QTF3, respectively. The QEPAS based sensor noise was determined as a standard deviation from the signal far from the targeted absorption line. The 1σ noise level was 4.81 μV, 4.76 μV, and 4.87 μV for QTF1, QTF2, and QTF3, respectively. The three all-fiber QEPAS sensors have almost the same signal and noise response. The signal-to-noise ratios (SNRs) calculated from the results measured were 46.3, 48.2, and 47.9. This resulted in a minimum detection limit (MDL) for H_2O of 99.4 ppm, 95.4 ppm, and

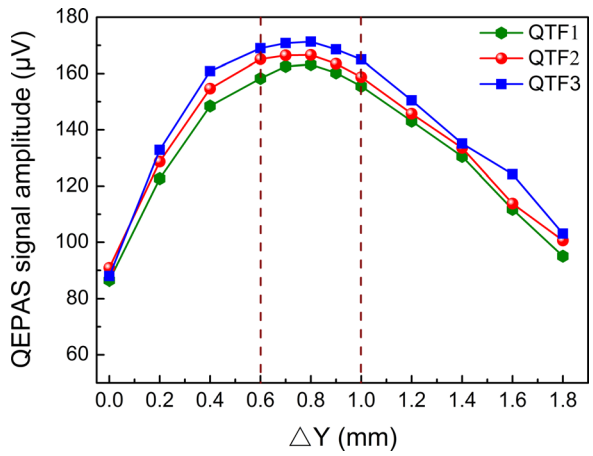

FIG. 2. All-fiber QEPAS sensor signal amplitude as a function of ΔY at a modulation depth of 0.39 cm^{-1} for the three sensors.

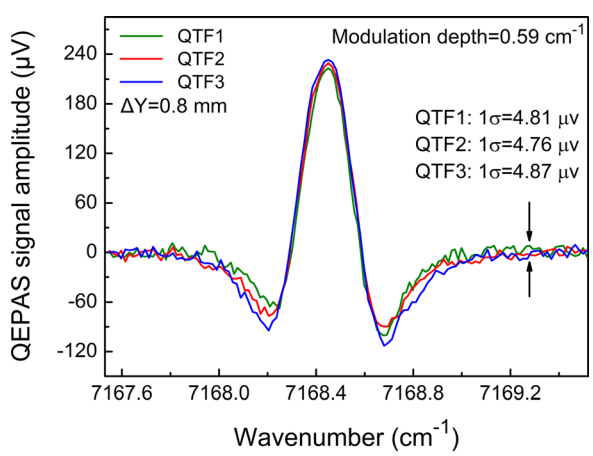

FIG. 4. 2*f* signal of the all-fiber QEPAS sensor system at ΔY of 0.8 mm and modulation depth of 0.59 cm^{-1}.

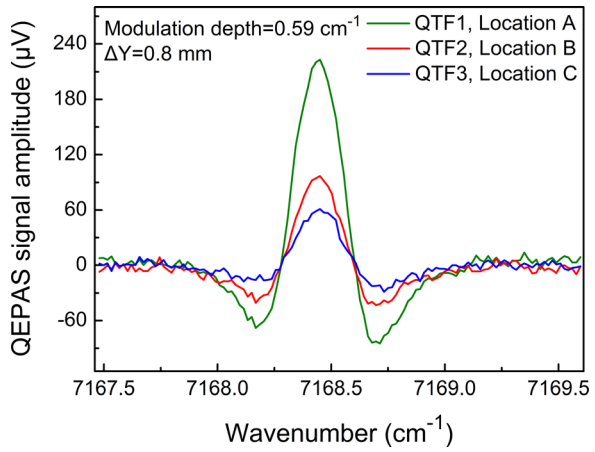

FIG. 5. H_2O detection for three different locations using the all-fiber QEPAS sensor.

96 ppm for QTF1, QTF2, and QTF3, respectively. The corresponding calculated normalized noise equivalent absorption coefficients (NNEA) were $1.11 \times 10^{-7}\,cm^{-1}\,W/\sqrt{Hz}$, $1.06 \times 10^{-7}\,cm^{-1}\,W/\sqrt{Hz}$, and $1.07 \times 10^{-7}\,cm^{-1}\,W/\sqrt{Hz}$, respectively.

H_2O detection at three different locations was performed to demonstrate the potential of spatially resolved trace gas concentration measurements. Locations A, B, and C were in three different cavities. The H_2O concentrations of the three different locations were controlled by changing the temperature and relative humidity. The measured results are shown in Fig. 5. The signal amplitude was 223 mV, 97 mV, and 61.1 mV for QTF1, QTF2, and QTF3, respectively. The H_2O concentration deduced from the measured QEPAS results were 0.46%, 0.20%, and 0.13% for location A, B, and C, respectively. This was also confirmed by means of the TDLAS method.

In conclusion, an ultra compact all-fiber H_2O QEPAS sensor using three QTFs with a resonance frequency of 30.72 kHz was demonstrated. Compared with conventional QEPAS using discrete optical components for laser delivery and coupling, the all-fiber configuration can reduce the sensor size to make it ultra compact. Furthermore, this all-fiber structure has other advantages, such as easier optical alignment, lower insertion loss, and lower cost. FBS was employed to split the laser beam into three sub sensor systems, and three QTFs were used for H_2O detection simultaneously to perform multi point detection. The MDL of 99.4 ppm, 95.4 ppm, and 96 ppm was achieved for QTF1, QTF2, and QTF3, respectively. The corresponding calculated NNEAs were $1.11 \times 10^{-7}\,cm^{-1}\,W/\sqrt{Hz}$, $1.06 \times 10^{-7}\,cm^{-1}\,W/\sqrt{Hz}$, and $1.07 \times 10^{-7}\,cm^{-1}\,W/\sqrt{Hz}$. Finally, simultaneously H_2O detection for three different locations was performed to demonstrate the potential of spatially resolved trace gas concentration measurements. The detection sensitivity of the all-fiber QEPAS based sensor system can be further improved by using an acoustic resonator.[13]

This work was supported by the National Natural Science Foundation of China (Grant Nos. 61505041 and 91441130), the Natural Science Foundation of Heilongjiang Province of China (Grant No. F2015011), the General Financial Grant from the China Postdoctoral Science Foundation (Grant No. 2014M560262), the Special Financial Grant from the China Postdoctoral Science Foundation (Grant No. 2015T80350), the Special Financial Grant from the Heilongjiang Province Postdoctoral Foundation (Grant No. LBH-TZ0602), the Financial Grant from the Heilongjiang Province Postdoctoral Foundation (Grant No. LBH-Z14074), the Fundamental Research Funds for the Central Universities (Grant No. HIT. NSRIF. 2015044), the National Key Scientific Instrument and Equipment Development Projects of China (Grant No. 2012YQ040164). Frank K. Tittel gratefully acknowledges the financial support from the U.S. National Science Foundation ERC MIRTHE award and a Grant No. C-0586 from the Welch Foundation.

[1]T. Mitsui, M. Miyamura, A. Matsunami, K. Kitagawa, and N. Arai, Clin. Chem. **43**(10), 1993 (1997).
[2]W. Ren, A. Farooq, D. F. Davidson, and R. K. Hanson, Appl. Phys. B **107**, 849 (2012).
[3]D. D. Arslanov, K. Swinkels, S. M. Cristescu, and F. J. M. Harren, Opt. Express **19**, 24078 (2011).
[4]A. Elia, P. M. Lugarà, C. di Franco, and V. Spagnolo, Sensors **9**, 9616 (2009).
[5]A. A. Kosterev, Y. A. Bakhirkin, R. F. Curl, and F. K. Tittel, Opt. Lett. **27**, 1902 (2002).
[6]L. Dong, V. Spagnolo, R. Lewicki, and F. K. Tittel, Opt. Express **19**, 24037 (2011).
[7]K. Liu, X. Y. Guo, H. M. Yi, W. D. Chen, W. J. Zhang, and X. M. Gao, Opt. Lett. **34**, 1594 (2009).
[8]M. Mordmüller, M. Köhring, W. Schade, and U. Willer, Appl. Phys. B **119**, 111 (2015).
[9]S. Borri, P. Patimisco, I. Galli, D. Mazzotti, G. Giusfredi, N. Akikusa, M. Yamanishi, G. Scamarcio, P. De Natale, and V. Spagnolo, Appl. Phys. Lett. **104**, 091114 (2014).
[10]H. M. Yi, R. Maamary, X. M. Gao, M. W. Sigrist, E. Fertein, and W. D. Chen, Appl. Phys. Lett. **106**, 101109 (2015).
[11]Y. F. Ma, R. Lewicki, M. Razeghi, and F. K. Tittel, Opt. Express **21**, 1008 (2013).
[12]X. Lin, X. L. Yu, F. Li, S. H. Zhang, J. G. Xin, and X. Y. Chang, Appl. Phys. B **110**, 401 (2013).
[13]L. Dong, A. A. Kosterev, D. Thomazy, and F. K. Tittel, Appl. Phys. B **100**, 627 (2010).